THE JOURNAL OF BIOLOGICAL CHEMISTRY VOL. 291, NO. 27, pp. 13918–13925, July 1, 2016

Direct Modulation of Heterotrimeric G Protein-coupled Signaling by a Receptor Kinase Complex*

Received for publication, May 6, 2016, and in revised form, May 26, 2016
Published, JBC Papers in Press, May 27, 2016, DOI 10.1074/jbc.C116.736702

Meral Tunc-Ozdemir[‡], Daisuke Urano[‡], Dinesh Kumar Jaiswal[‡], Steven D. Clouse[§], and Alan M. Jones[‡¶1]

From the Departments of [‡]Biology and [¶]Pharmacology, University of North Carolina, Chapel Hill, North Carolina 27599 and the [§]Department of Horticultural Science, North Carolina State University, Raleigh, North Carolina 27695-7609

Plants and some protists have heterotrimeric G protein complexes that activate spontaneously without canonical G protein-coupled receptors (GPCRs). In *Arabidopsis*, the sole 7-transmembrane regulator of G protein signaling 1 (AtRGS1) modulates the G protein complex by keeping it in the resting state (GDP-bound). However, it remains unknown how a myriad of biological responses is achieved with a single G protein modulator. We propose that in complete contrast to G protein activation in animals, plant leucine-rich repeat receptor-like kinases (LRR RLKs), not GPCRs, provide this discrimination through phosphorylation of AtRGS1 in a ligand-dependent manner. G protein signaling is directly activated by the pathogen-associated molecular pattern flagellin peptide 22 through its LRR RLK, FLS2, and co-receptor BAK1.

In *Arabidopsis thaliana* (hereafter referred to as *Arabidopsis*), the heterotrimeric G protein complex consists of one canonical Gα subunit (AtGPA1), one Gβ subunit (AGB1), and one of three Gγ subunits (AGG1, AGG2, and AGG3) (1). The canonical Gα subunit AtGPA1 self-activates through spontaneous GDP/GTP exchange without G protein-coupled receptors (GPCRs)[2] (2). Gα activation is followed by structural rearrangements enabling interaction with downstream target proteins (3). AtRGS1 is a negative regulator, having a GPCR-like N-terminal seven-transmembrane domain fused to a regulator of G protein signaling (RGS) protein, which keeps the G protein complex in the inactive state (4). This is in contrast to animals, where nucleotide exchange is the rate-limiting step catalyzed by its cognate GPCR. In animals, continued agonist occupancy of the GPCR leads to phosphorylation at its cytoplasmic C-terminal domain, leading to desensitization through GPCR endocytosis, whereas in *Arabidopsis*, agonist-induced endocytosis of AtRGS1 leads to sustained activation. Phosphorylation of GPCRs and AtRGS1 is necessary and sufficient for their endocytosis (5, 6). In *Arabidopsis*, glucose-induced endocytosis of AtRGS1 is initiated by its transphosphorylation by three with no lysine (WNK) kinases (7, 8). AtRGS1 endocytosis physically uncouples the GTPase-accelerating activity of AtRGS1 from the Gα protein, allowing spontaneous nucleotide exchange and sustained activation (8). Therefore, AtRGS1 serves as a key point of ligand-dependent signal modulation of heterotrimeric G proteins.

We proposed that plant G protein activation may be modulated in a non-conventional manner through other discriminators, perhaps serving as co-receptors to AtRGS1 (9). *Arabidopsis* has more than 400 receptor-like kinases (RLKs) consisting of an extracellular domain, each potentially recognizing one among a wide range of ligands, a single-pass transmembrane domain, and a cytoplasmic kinase domain having homology to the *Drosophila* Pelle family of kinases (10–12). Accumulating genetic evidence suggests that some of these RLKs serve as receptors or co-receptors in G protein-coupled signaling in plants to mediate proper development, pathogen defense, and cell death (13–18); however, there is no direct biochemical evidence to support this idea.

Heterotrimeric G proteins play a role in defense responses in which pathogen-associated molecular patterns (PAMPS) signals bind leucine-rich repeat (LRR) RLKs to generate reactive oxygen species and to activate immunity pathways such as MAP kinase cascades (19, 20). We hypothesized that specific LRR RLKs directly modulate G signaling through phosphorylation of AtRGS1 to induce its endocytosis and thus consequently release its inhibition on G protein self-activation. In this study, we screened 70 LRR RLKs to determine whether AtRGS1 serves as an LRR RLK substrate. LRR RLKs identified in this screen led us to elucidate the mechanism of direct activation of G signaling by a receptor kinase, previously unknown for the heterotrimeric G protein pathway.

Results

Receptor-like Kinase Phosphorylation of AtRGS1—The *Arabidopsis* genome has more than 200 LRR RLK subfamily members (21). Many LRR RLKs are well known including their three-dimensional structures, cognate ligands, kinase domain substrates, and autophosphorylation sites (22–24). The G protein complex and several plant LRR RLKs cooperatively control plant development, cell death, and responses to biotic and abiotic stress; however, the molecular mechanism of the cooperation remains poorly understood. To test the hypothesis that LRR RLKs directly activate G protein by phosphorylating its negative regulator AtRGS1, we screened 70 active, recombi-

* This work was supported by NIGMS, National Institutes of Health Grant R01GM065989 and National Science Foundation (NSF) Grant MCB-0718202 (to A. M. J), and NSF Grant MCB-1021363 (to S. D. C.). The Division of Chemical Sciences, Geosciences, and Biosciences, Office of Basic Energy Sciences of the U. S. Department of Energy through Grant DE-FG02-05er15671 (to A. M. J.) funded technical support in this study. The authors declare that they have no conflicts of interest with the contents of this article. The content is solely the responsibility of the authors and does not necessarily represent the official views of the National Institutes of Health.
[1] To whom correspondence should be addressed: Dept. of Biology, CB# 3280, University of North Carolina, Chapel Hill, NC 27599-3280. Tel.: 919-962-6932; Fax: 919-962-1625; E-mail: alan_jones@unc.edu.
[2] The abbreviations used are: GPCR, G protein-coupled receptor; RGS, regulator of G protein signaling; LRR RLK, leucine-rich repeat receptor-like kinase; BAK1, BRI1-associated kinase; PAMP, pathogen-associated molecular pattern; DDM, *n*-dodecyl-β-D-maltoside; Ct, C-terminal tail; pS, phosphorylated serine.

nant arginine-aspartate-type LRR RLKs (22) (Fig. 1, *A* and *B*). The levels of trans- and autophosphorylation were quantitated (data not shown) and found not to correlate, statistically supported by a correlation coefficient $R^2 = 0.01$. For example in Fig. 1*A*, reaction #29 (At4G20140) showed autophosphorylation but poor AtRGS1 transphosphorylation. At the other extreme, reaction #52 (At2G28970) transphosphorylated AtRGS1 but autophosphorylated weakly. Moreover, because the majority of kinases, each purified under the same conditions, did not phosphorylate AtRGS1, a contaminating kinase from *Escherichia coli* is excluded as the source of phosphorylation. Other negative controls were reactions with no kinase (*NC*, Fig. 1*A*) and a kinase-dead LRR RLK At1g29440 (reaction #70, Fig. 1*A*).

Among the tested LRR RLKs that phosphorylated AtRGS1 *in vitro*, several are involved in pathogen defense such as BAK1-like 1 (BKK1) (25, 26), PEP1 receptor 1 (27), and impaired oomycete susceptibility 1 (IOS1) (28). As depicted in Fig. 1*B*, each of these LRR RLKs heterodimerize with brassinosteroid-associated kinase (BAK1) (29, 30) and are required for PAMP-triggered immunity, cell death, and development (31–33). BAK1 also interacts with two other receptors: flagellin-sensing 2 (FLS2), which binds the PAMP flg22 (22-amino acid peptide from flagellin), and BAK1-interacting receptor 1 (BIR1), which genetically interacts with heterotrimeric G proteins in flg22-initiated innate immunity and cell death (34–36). BAK1 and FLS2 were not in the original set of screened LRR RLKs; therefore they are included in a second test of the transphosphorylation of AtRGS1, following reaction optimization. Transphosphorylation of AtRGS1 by BKK1 and IOS1 was confirmed by the second screen; BAK1 strongly phosphorylated AtRGS1; and neither BIR1 nor FLS2 phosphorylated AtRGS1 under this test condition (Fig. 1*C*). Note that we observed no autophosphorylation of FLS2 in contrast to Gómez-Gómez *et al.* (37). Liquid chromatography-tandem mass spectrometry analysis of recombinant RGS box + Ct (Fig. 1*D*) phosphorylated by BAK1 identified one phosphorylation site, Ser^{428} (Fig. 1, *E* and *F*) in the entire AtRGS1 C-terminal domain. Sequence coverage identified by mass spectrometry was excellent, and the three fragments not identified lacked Ser and Thr (Fig. 1*E*). The identified phosphorylated tryptic peptide is shown in Fig. 1*F*. Because the stoichiometry under the tested conditions was 0.5 mol of phosphate/mol of AtRGS1 C-terminal domain (data not shown), Ser^{428} is likely the sole amino acid in the AtRGS1 C-terminal domain phosphorylated by BAK1.

BAK1 is a partner to the flg22 receptor FLS2. Therefore, we tested the effect of flg22 on AtRGS1 phosphorylation *in vivo* using a phospho-specific antibody against Ser^{428} and two other known phosphorylation sites, Ser^{435} and Ser^{436} (8). As shown in Fig. 1*G*, flg22 increased by 2-fold the pool of phosphorylated native AtRGS1 (the *bottom band* to the *right* of the *arrow* is the native AtRGS1 having ~50 kDa of molecular mass) and YFP-tagged AtRGS1 (the *upper band* shows ~70 kDa of YFP-tagged AtRGS1) within a 5-min exposure to 100 nM flg22 in stably transformed *Arabidopsis* wild type expressing YFP-tagged AtRGS1. As will be elaborated later, a 2-fold increase in the phosphorylated pool is consistent with a cellular change in AtRGS1. The flg22 effect requires its receptor FLS2 because the *fls2* null mutant lacked phosphorylated AtRGS1 (Fig. 1*G*). Because seven-transmembrane proteins are notoriously difficult to extract, we used two different detergents, *n*-dodecyl-β-D-maltoside (DDM) and ASB-14, that are effective in AtRGS1 solubilization (38). ASB-14-solubilized AtRGS1 is shown in Fig. 1*G*, but similar results for DDM-solubilized AtRGS1 were also observed (data not shown). Among the many LRR RLK candidates that emerged from our screen, we chose the flg22/FLS2 pathway to test LRR RLK activation of G signaling.

Direct Activation of a G Protein by a Receptor Kinase—Ideally, to quantitate direct G protein activation, one would quantitate changes in intermolecular FRET efficiency between donor and acceptor fluorophores within the heterotrimeric G protein complex, but this is not possible (39).[3] Therefore, in lieu of a Gα-Gβγ FRET reporter, there are two standardized reporters for plant G protein activation: 1) FRET efficiency change between AtRGS1-YFP and AtGPA1-CFP reports maximum glucose-induced activation at 4 min and its return to the starting level within 8 more min (40), and 2) endocytosis of AtRGS1 reports sustained G protein activation in the 10–30-min time range (7).

To test the hypothesis that flg22/FLS2/BAK1 directly activates G protein-coupled signaling in plants, we first measured the FRET efficiency changes between AtRGS1-YFP and AtGPA1-CFP in response to flg22. A low concentration of flg22 (100 nM) as well as a higher one (1 μM) decreased FRET efficiency between AtRGS1-YFP and AtGPA1-CFP to zero within 5 min (Fig. 2*A*, $p < 0.05$), indicating a large proximity change between these two proteins. By 10 min after flg22 addition, FRET efficiency returned toward the starting level. The strength and timing were the same observed as for glucose-induced changes in FRET efficiency (40). When the cells were treated with the phosphatase inhibitor calyculin A prior to flg22 treatment, the return to baseline was delayed, indicating that the phosphorylation state of AtRGS1 is associated with the flg22-induced conformational change (Fig. 2*A*).

Because phosphorylation of AtRGS1 at the C-terminal Ser^{428} is necessary for endocytosis by WNK8 kinase in response to D-glucose (8), we hypothesized that AtRGS1 phosphorylation by LRR RLKs at Ser^{428} results in endocytosis in response to its cognate ligand, leading to physical uncoupling of Gα protein from AtRGS1 and, consequently, activation of G signaling. To test this hypothesis, we quantitated G protein activation induced by flg22 by analyzing the percentage of AtRGS1 endocytosis over time in *Arabidopsis* hypocotyls (Fig. 2*B*). flg22 (1 μM) internalized ~55% of AtRGS1 within 3 min ($p < 0.01$). The flg22 effect is structurally specific because mutation of the flg22 peptide (ΔFLG22 flg15-Δ7; sequence RINSAKDD (41)) failed to induce AtRGS1-YFP internalization at the same concentration (Fig. 2*B*, *inset*). The observed changes in the percentage of internalized AtRGS1 over time are consistent with the flg22-induced change in the AtRGS1 phosphorylation state. Specifically, given the fact that the stoichiometry of phosphate to AtRGS1 determined *in vitro* is ~1 and given that flg22 induces an ~2-fold increment in AtRGS1 internalization, the observed

[3] M. Tunc-Ozdemir and A. M. Jones, unpublished data.

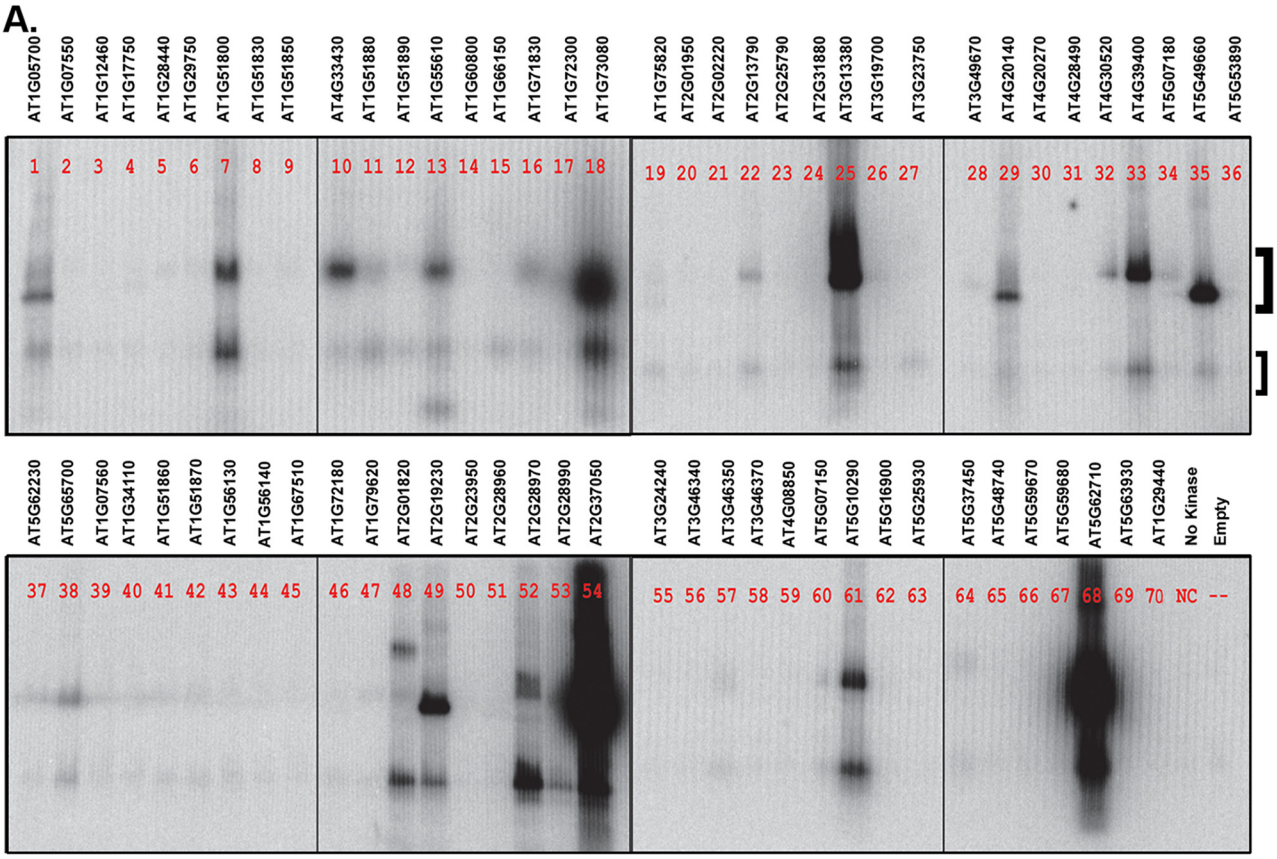

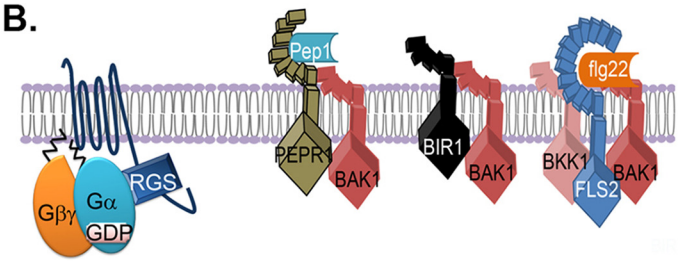

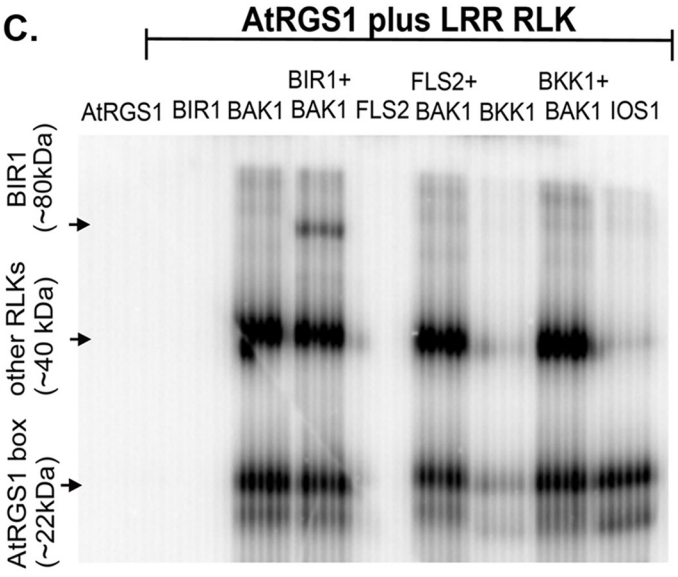

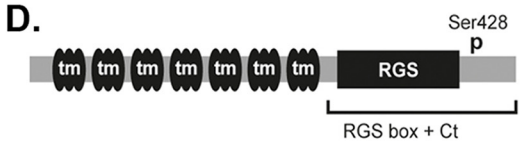

E. KEEFRPV DPNEPLDKLLLNKRFRHSFM EFADSCYAGE TLHFFEEVYEHGKIPEDDSIRRIYMARHIMEKFIVAGAEM ELNLSHKTRQ EILTTQDLTHTDLFKNALNEVMQLIKMNLV RDYWSSIYFI KFKEEESCHEAMHKEGYSFSSPRLSSVQ GS DDPFYQEHMSKSSRCSSPG

F. 425E G Y S F S S P R433

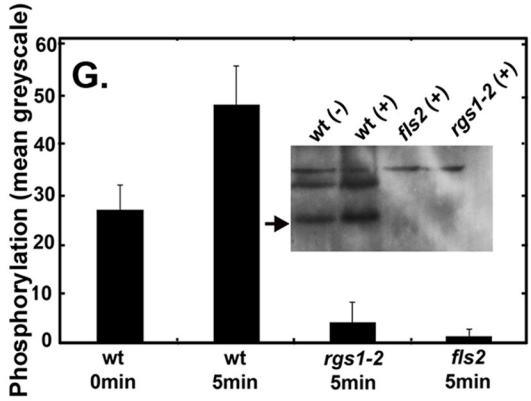

2-fold difference in flg22-induced phosphorylated AtRGS1 meets expectation (Fig. 1*F*). When the C-terminal domain containing the phosphorylation motifs was truncated (Fig. 2*C*) or when Ser^{428} on AtRGS1 was mutated (Fig. 2*D*), the 1 μM flg22 did not induce internalization of AtRGS1-YFP.

flg22-induced endocytosis of AtRGS1-YFP was also impaired in the *fls2* (Fig. 2*B*) and *bak1-4* (Fig. 2*E*) mutants treated with 1 μM flg22, indicating that FLS2/BAK1 are the co-receptors for flg22 activation of G signaling. To confirm that AtRGS1 endocytosis was still feasible in the *fls2* or *bak1-4* mutants, glucose was tested, and we found that the previously reported internalization (8) occurred at 30 min in both *bak1-4* (Fig. 2*E*) and *fls2* mutants (data not shown). The lack of a flg22-increased phosphorylation of AtRGS1 in *bak1-4* mutants as seen in the wild type (Fig. 2*F*) indicates that BAK1 is required for flg22-dependent G signaling activation.

Discussion

Discrimination of signals achieved via GPCRs in animal heterotrimeric G signaling pathways is well understood (42, 43). However, for plants that lack GPCRs, such clarity was missing despite the evidence to date indicating that many different signals are coupled by the plant G protein complex to cellular responses (2, 9, 40, 44). Our results suggest that signal specificity achieved in plant cells generally occurs directly through AtRGS1 phosphorylation by LRR RLKs.

There are three possible mechanisms for how the phosphorylation of the AtRGS1 domain alters the function of the system, and we confirmed one. 1) Phosphorylation of AtRGS1 alters the global conformation to its Gα substrate and by doing so is no longer able to accelerate the intrinsic GTPase activity, and thus Gα self-activates. We showed that this conformational change occurs (Fig. 2*A*). 2) flg22 directly inhibits AtRGS1 catalytic GAP activity, although this mechanism is unlikely because flg22 acts extracellularly yet the RGS catalytic domain is cytoplasmic. Nonetheless, this mechanism remains a possibility as we have not yet tested the GAP activity of a phosphorylated AtRGS1. 3) The adaptor requires AtRGS1 to be phosphorylated before it can interact with it to commence endocytosis, similar to GPCR endocytosis requiring their cognate adaptors, β-arrestins. To test this hypothesis, we need to know the adaptor. There are no β-arrestins in plant cells, but there are candidate arrestin-fold proteins (45) to be tested in follow-on studies. We do not exclude the possibility that the role of AtRGS1 phosphorylation in the G protein activation mechanism is also required for adaptor recognition.

Given that all the LRR RLKs that are known to operate in innate immunity either phosphorylate AtRGS1 *in vitro* or genetically interact with BAK1, we speculate that BAK1/co-receptor itself provides the discrimination of signal to G proteins. A study of two BAK1 mutants suggested that varied phosphorylation patterns of RLK partners (BRI1, FLS2, EFR, and BIK1) by BAK1 is the basis for selective regulation of signaling pathways (46, 47). Thus, we speculate that phosphorylation of different AtRGS1 residues by BAK1 in response to different signals may drive diverse functions of heterotrimeric G proteins in plant development, defense, cell death, and biotic stress response pathways.

At present, our data do not distinguish between AtRGS1 internalization 1) being the starting point for a signal downstream on the endosomes by itself or along with FLS2, 2) being part of the desensitization of LRR RLK activation, or 3) being solely important for G protein activation as it is an inhibitor of the complex on the membrane. If it is the former, AtRGS1 endocytosis with the different receptors in different signaling pathways could explain the signal specificity achieved downstream of the activation complexes formed by AtRGS1. In addition, BAK1 or the other LRR RLKs might phosphorylate AtRGS1 at different sites, and this might change the specificity of downstream signaling or in which complex AtRGS1 would be endocytosed. These are unresolved questions for future studies.

We do not exclude the possibility that BAK1 has other phosphorylation targets than AtRGS1. By precedent, the yeast Gα subunit is phosphorylated by a non-receptor kinase in response to changes in the cell cycle (48) and is also phosphorylated in response to the limited availability of glucose (49). Also, in the membranes of human leukemia HL-60 cells during activation of G proteins, the Gβ subunit is phosphorylated (50). It is also possible by analogy that RLKs phosphorylate other components of the G protein complex. Recently, Liang *et al.* (51) showed that BIK1, a cytoplasmic kinase, phosphorylates an extra large isoform of the Gα subunit.

Experimental Procedures

Plant Materials—Arabidopsis Col-0 and T-DNA insertion null mutants *rgs1-2* (SALK_074376.55.00) (4) and *fls2* (SAIL_691_C4) (53) plants were grown in soil under fluores-

FIGURE 1. **Various LRR-RLKs phosphorylate AtRGS1.** *A*, *in vitro* kinase reactions with 70 LRR RLKs (Mitra *et al.* (22)) were performed as described under "Experimental Procedures." Reaction numbers are indicated in *red*. Shown are autoradiographs of [γ-^{32}P]ATP-phosphorylated AtRGS1 and LRR RLK (top band in each lane), and the TAIR (The Arabidopsis Information Resource) locus number of the reaction RLK is provided above the lanes. Eight independent gels are shown. The *top bracket* shows the migration range of 40–60-kDa proteins, and the *bottom bracket* shows ~20-kDa proteins for independent gels. *B*, several of the LRR RLKs that phosphorylate AtRGS1 identified in the screen shown in *panel A* heterodimerize with the LRR RLK BAK1 (*red kinase*): FLS2, BKK1, PEP1 receptor 1 (PEPR1), BIR1, and IOS1. At the *left* is the G protein complex containing the G$\alpha\beta\gamma$ subunits and AtRGS1. *C*, phosphorylation of AtRGS1 by BAK1. Radioactivity from γ-^{32}P was digitally quantitated by PhosphorImager (GE/Amersham) showing *in vitro* phosphorylation of the AtRGS1 C-terminal domain by selected RLKs (BAK1, FLS2, BIR1, BKK1, and IOS1 individually and with BAK1). The *upper two arrows* indicate the autophosphorylated LRR RLK. BIR1 and FLS2 lacked autophosphorylation activity under the conditions used here. AtRGS1 in *lane 1* is a negative control. *D*, full-length AtRGS1 illustration showing the 7-transmembrane (*TM*) helices, the RGS box domain, the Ct, and a previously known phosphorylated Ser^{428} (8). *E*, phospho-mapping sequence coverage. Tryptic peptides of the RGS box + C-terminal protein phosphorylated by BAK1 were subjected to LC-MS/MS analysis. *Green sequences* are detected peptides from complete and partial digestion. The detected phosphorylation site (Ser^{428}) is shown in *red*. Sequences in *black* were not detected. *F*, fragments identified in MS used to assign the phosphate adjunct to Ser^{428}. *y* and *b* ions are indicated by the *breaks*. *G*, flg22 induces AtRGS1 phosphorylation *in vivo*. 35S:AtRGS1-YFP was expressed in wild type or *fls2* plants. After 100 nM flg22 treatment of 10-day-old seedlings for 5 min, AtRGS1 phosphorylation was detected by immunoblotting with an anti-phospho-AtRGS1 antibody. The intensity of the native AtRGS1 phosphorylation bands was quantified by ImageJ software, and the percentage of their ratio is shown. Statistics are based on three replicates. *Error bars* represent S.E. *Inset*, the largest band is background because it is found in all samples. The second largest band recognized by the anti-phospho-AtRGS1 antibody is the AtRGS1-YFP. The *arrow* shows a protein of the size of native AtRGS1 recognized by the anti-phospho-RGS1 antibody.

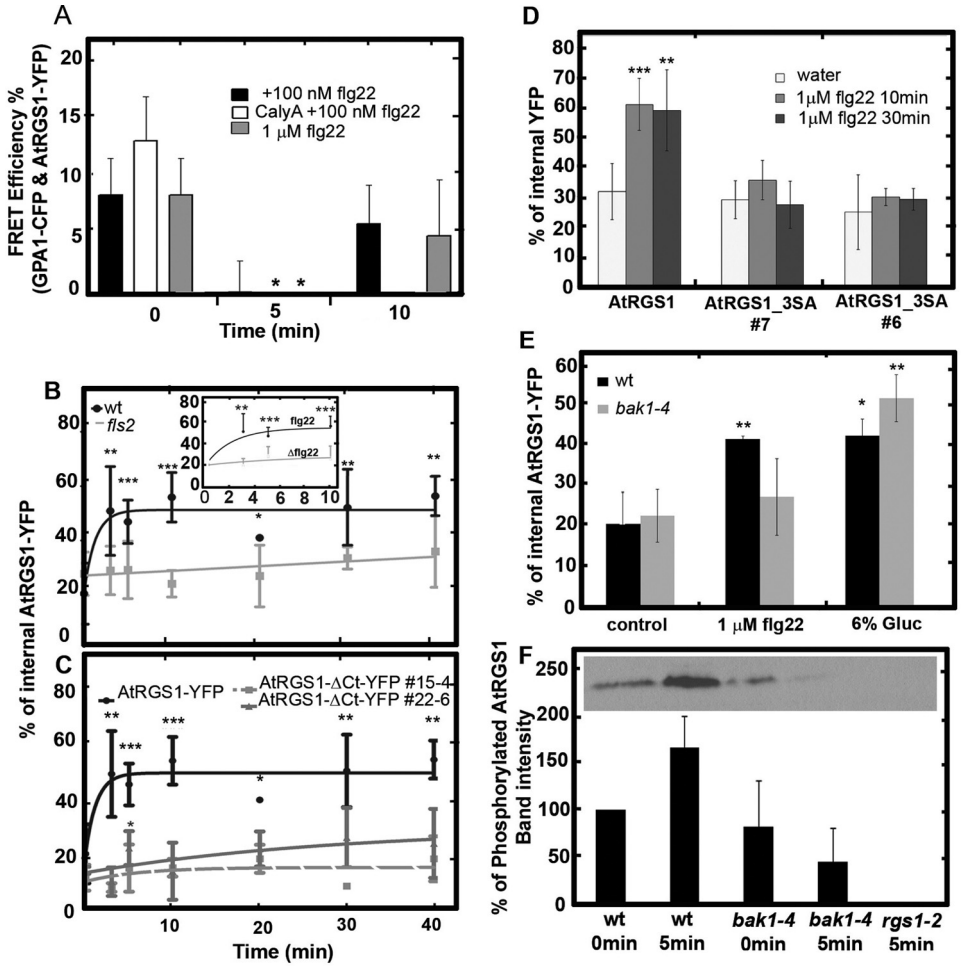

FIGURE 2. **Heterotrimeric G protein complex is directly activated by phosphorylation-dependent flg22 signaling.** *A*, flg22 activates G signaling *in vivo*. flg22-induced changes in AtGPA1 and AtRGS1 interaction in *Nicotiana benthamiana* were detected. Changes in FRET efficiency ((the fluorescence intensity of the donor (CFP) after acceptor photobleaching (Dpost) − the fluorescence intensity of the donor before acceptor photobleaching/Dpost)) of *N. benthamiana* cells expressing *GPA1-CFP* and *AtRGS1-YFP* in the presence of 100 nM (*black bar*) or 1 μM flg22 (*gray bar*) were detected. A 40-min pretreatment of 100 nM calyculin A (*CalyA*) was followed with a 100 nM flg22 treatment for calyculin A + 100 nM flg22 samples (*white bar*). *Error bars* represent S.E. of regions of interest ($n = 3–9$). *B*, flg22 activates sustained G signaling in an FLS2-dependent manner. AtRGS1 internalization in hypocotyls of wild type (*black line*, *solid circles*) or *fls2* (*gray line*, *solid squares*) plants expressing AtRGS1-YFP is shown over time. The *inset* shows an expanded time range between 0 and 10 min after flg22 addition. Δflg22 is the negative control peptide (*lower gray line* indicates flat response). *Error bars* represent standard deviation of AtRGS1 internalization in 3–8 hypocotyl epidermal cells from two experiments. *C*, truncation of the phosphorylation motif on AtRGS1 abrogates flg22-induced internalization of AtRGS1. Internalization of AtRGS1-YFP *versus* AtRGS1ΔCt-YFP (two transgenic lines #15-4 and 22-6, *solid* and *dashed gray lines*) in response to 1 μM flg22 is shown over time. The data of the AtRGS1-YFP from *panel B* were replotted. *Error bars* represent standard deviation of AtRGS1 internalization in 3–8 hypocotyls. *D*, mutation of Ser^{428} to Ala abrogates flg22-induces AtRGS1 endocytosis. Two independent lines expressing RGS1 (S428A,S435A,S436A "AtRGS1_3SA") mutant tagged with YFP in the *rgs1* null background (#6 and #7) were tested. AtRGS1_3SA is not endocytosed by flg22, unlike the wild type protein (AtRGS1). Two time points are shown. *Error bars* represent S.D. *E*, BAK1 is required for AtRGS1 endocytosis in response to flg22. AtRGS1 internalization in hypocotyl epidermal cells of wild type (*black bars*) or *bak1-4* (*gray bars*) plants expressing AtRGS1-YFP was measured after 10 min of 1 μM flg22 or 30 min after 6% glucose addition. *Error bars* represent standard deviation of AtRGS1 internalization in 3–8 hypocotyl epidermal cells. *F*, flg22-induced AtRGS1 phosphorylation *in vivo* depends on BAK1. 35S:AtRGS1-YFP was expressed in wild type or *bak1-4* plants. AtRGS1 phosphorylation of 6-week-old seedlings was detected by immunoblotting with an anti-phospho-AtRGS1 antibody upon 5 min of 100 nM flg22 treatment via infiltration with a needless syringe. (The *inset* shows the Western blot of one experiment.) Phosphorylated AtRGS1-YFP is recognized by an anti-phospho-RGS1 antibody described by Urano *et al.* (8). The intensity of the AtRGS1 phosphorylation bands from replicated experiments was quantified by Adobe Photoshop, and the average *gray* mean values of bands detected in two biological replicates were plotted with the S.E. Values between control and treatment or mutant groups were statistically examined by the Student's *t* test. *, **, or *** represent differences from the control groups at the *p* values of 0.05, 0.01, or 0.001, respectively.

cent lights (12 h of light (150 microeinstein/m^2/s) and 12 h of dark) at 23 °C.

Protein Purification for the in Vitro Screen of AtRGS1 Phosphorylation by RLKs—cDNAs encoding the complete cytoplasmic domain (juxtamembrane region, catalytic kinase domain, and C-terminal region) for each *Arabidopsis* LRR RLK were cloned into a modified pET Gateway vector for expression of His-tagged recombinant protein in *E. coli* BL21 (DE3) pLysS cells (22). After culture at 37 °C for 2 h, expression of the kinase domains was induced in BL21 cells with 0.5 mM isopropyl-β-thiogalactopyranoside at 28 °C for 4 h (A_{600} 0.6–0.8). The pellet was suspended in 1.5 ml of extraction buffer (50 mM Tris-HCl (pH 8.0), 100 mM NaCl, 1 mM $MgCl_2$, 2 mM 2-mercaptoethanol, 1 mM PMSF, and 1 μg/ml leupeptin). Lysozyme, Nonidet P-40, and DNase I were then added to final concentrations of 1.25 mg/ml, 0.5%, and 25 μg/ml, respectively. The suspension was rocked for 1 h at 4 °C, and then spun with a tabletop centrifuge for 10 min at 4 °C. The supernatant was mixed with 50 μl of TALON and 50 μl of extraction buffer including 20 mM imidazole. The solution was placed on a tumbling table at 4 °C over-

night. The tubes were centrifuged to pellet the TALON resin, which was transferred to a mini spin column. The resin was washed with wash buffer (50 mM Tris-HCl (pH 8.0), 500 mM NaCl, 2 mM imidazole, 1 mM $MgCl_2$, 2 mM 2-mercaptoethanol, and 1 mM PMSF). Kinase proteins were eluted with 200 μl of elution buffer (25 mM Tris-HCl (pH 8.0), 250 mM NaCl, 1 M imidazole, 0.5 mM $MgCl_2$, 1 mM DTT, and 1 mM PMSF). SDS-PAGE was used to determine protein purity. The eluted solution was dialyzed with dialysis buffer (10 mM Tris-HCl (pH 7.5), 20 mM NaCl, 1 mM DTT, and 1 mM PMSF). 200 μl of kinase solution was then mixed with 100 μl of 50% glycerol in elution buffer, and then flash-frozen using liquid nitrogen. Protein concentrations were determined with the Bradford assay. The His_6-tagged RGS1 cytoplasmic region was prepared as described (8).

In Vitro Phosphorylation Assay—Purified kinase protein was mixed with His_6-tagged AtRGS1 C-terminal domain (His_6-RGS box + Ct, residues from 284 to 459) protein in 25 μl of reaction buffer (50 mM Tris-HCl (pH 7.5), 10 mM $MgCl_2$, 10 mM $MnCl_2$, 1 mM DTT, 1 μg/ml leupeptin, 0.1 μM calyculin A, and 50 μM ATP (including 2 μCi of radiolabeled [γ-^{32}P]ATP at 3,000 Ci/mmol)), and then incubated at room temperature for 8.5 h. Approximately 1 μg of kinase domain and 2.7 μg of His_6-RGS-box + Ct were added into each reaction. The reaction was stopped by adding 10 μl of 5× Laemmli sample buffer. The kinase and His_6-RGS + Ct proteins were separated on an SDS-PAGE gel, and the radiolabeled phosphate transferred on proteins was visualized with the phospho-image analyzer.

In Vivo AtRGS1 Phosphorylation Assays—To examine the phosphorylation of AtRGS1 in *Arabidopsis* plants, ~200 wild type and *fls2* seedlings expressing 35S:AtRGS1-YFP and *rgs1-2* mutants were grown at continuous dim light (30–50 microeinsteins/m^2/s) at 22 °C for 10 days, and then they were treated with 0 or 100 nM flg22 for 5 min. For *bak1-4*-related phosphorylation experiments, the leaves of 6-week-old plants expressing 35S:AtRGS1-YFP grown in soil under fluorescent lights (12 h of light (150 microeinsteins/m^2/s) and 12 h of dark) at 23 °C were infiltrated with water or 100 nM flg22 before harvest. Whole tissue for seedlings and leaf tissue for 6-week-old plants were harvested and ground in liquid nitrogen. Total plant crude extracts were prepared with 10 ml of grinding buffer (50 mM Tris-HCl (pH 8.0), 150 mM NaCl, 10 mM EDTA, 1 mM PMSF, 2 mM DTT, and 1× plant protease inhibitor cocktail (Sigma-Aldrich)). The lysates were centrifuged at 12,000 × *g* for 15 min at 4 °C after cell debris was removed from the homogenate by filtration through one-layered Miracloth (Calbiochem). Supernatants were collected, and then the concentration was determined with the Bio-Rad Bradford quantification. The supernatant was recovered and centrifuged at 100,000 × *g* for 30 min at 4 °C. The membrane fraction was suspended in buffer containing 50 mM Tris-HCl (pH 8.0), 150 mM NaCl, 10 mM EDTA, 1 mM PMSF, 2 mM DTT, and 1% ASB-14 or 1% DDM.

Protein extracts were electrophoresed through 10% SDS-PAGE, followed by immunoblot analysis (4 °C overnight incubation using a 1:2000 dilution of purified anti-phospho-AtRGS1 directed against amino acids 424–440: CKEGY-pS-FSSPRL-pS-pS-VQGS (pS; phosphorylated serine; YenZym Antibodies) antibody described in Ref. (8) in 1× TBST buffer (50 mM Tris-Cl, pH 7.6; 150 mM NaCl, and 2.5% Tween 20)). Blots were reacted with peroxidase conjugated to IgG fraction of monoclonal mouse light chain-specific anti-rabbit at a dilution of 1:10,000 (Jackson ImmunoResearch) in 2.5% milk dissolved in 1× TBST buffer and then detected by ECL or ECL Plus, following the manufacturer's guidance (GE Healthcare, Amersham Biosciences). For semi-quantification of phosphorylation, we normalized signal intensity of the related bands to total protein loading (assessed by staining of membranes using Coomassie Blue and Ponceau stains).

Identification of Phosphorylation Site by Mass Spectrometry—The AtRGS1 protein (RGS box + Ct) was purified and phosphorylated *in vitro* using BAK1 kinase as described above. The kinase reactions were loaded on a 12% SDS-polyacrylamide gel and visualized using Coomassie Blue staining. The corresponding bands in the gel were manually excised and subjected to in-gel trypsin digestion. Phosphorylated peptides were enriched using a titanium dioxide (TiO_2) column, and MS3 spectra of phosphorylation sites were recorded on an LTQ-Orbitrap XL (Thermo Scientific) and Q Exactive HF mass spectrometer (Thermo Scientific) as described earlier (54). Both phosphopeptide-enriched and non-phosphopeptide fractions (flow-through) were analyzed by mass spectrometry. Raw spectra were processed using the Proteome Discoverer software, and the identities of peptide and protein, as well as the phosphorylation sites, were mapped.

G Protein Activation Assays—Stable *Arabidopsis* lines expressing AtRGS1-YFP and AtGPA1 with CFP inserted in a plant-specific loop at amino acid 97 (40) were used for the Förster resonance energy transfer (FRET acceptor photobleaching-based assay essentially as described by Ref. 52). Briefly, 514 and 458 nm argon lasers were tuned to excite YFP (acceptor) and CFP (donor), respectively. Acceptor and donor channel emissions were detected within the ranges of 516–596 and 460–517 nm, respectively Regions of interest were scanned five times each using a 514 nm argon laser line at 100% intensity with a pinhole diameter set to 1.00 airy unit so that the acceptor was photobleached to ~20–50% of its initial value.

Internalization assays were performed according to Fu *et al.* (7). Briefly, wild type, *fls2*, or *bak1-4* plants transformed with AtRGS1-YFP, AtRGS1-3SA-YFP (in which the known phosphorylation sites (Ser^{428} and Ser^{435}/Ser^{436}) located in the C-terminal tail of AtRGS1 were mutated), or AtRGS1ΔCt-YFP were grown in liquid half-strength MS medium for 4–6 days in the dark. Hypocotyl epidermal cells located 2–4 mm below the cotyledons of seedlings treated with water, flg22, Δflg22, or 6% glucose were imaged with a Zeiss LSM710 confocal laser scanning microscope with C-Apochromat × 40/1.2 water immersion objective. A 489 nm diode laser was tuned to excite YFP, and emission was detected at 526–563 nm by a photomultiplier tube detector. A z stack series of ~15 multiple focal plane images at 0.5-μm steps, starting from the apical plasma membrane, was taken. Images acquired about ~2–3 μm below the top layer of cells in the Z plane were used to quantify the AtRGS1 endocytosis fraction (vesicular structures in the cytoplasm with YFP signal) after images were converted to 8-bit. and a threshold was chosen for fluorescence signal using

ImageJ. Regions of cells were determined based on the outlines of cells in the corresponding bright-field image.

Author Contributions—Author contributions: M. T-O. conducted the FRET, AtRGS1 internalization, and *in vivo* phosphorylation experiments, analyzed the results, and edited the manuscript. D. U. conceived the idea for the project and along with D. K. J. performed the biochemistry assays and edited the manuscript. S. D. C. provided critical unpublished reagents that enabled the project. A. M. J. managed the project and wrote the manuscript.

Acknowledgments—This research is based in part upon work conducted using the UNC Michael Hooker Proteomics Center, which is supported in part by the National Institutes of Health-NCI Grant CA016086 to the Lineberger Comprehensive Cancer Center.

References

1. Thung, L., Trusov, Y., Chakravorty, D., and Botella, J. R. (2012) Gγ1 + Gγ2 + Gγ3 = Gβ: the search for heterotrimeric G-protein γ subunits in *Arabidopsis* is over. *J. Plant Physiol.* **169,** 542–545
2. Urano, D., Jones, J. C., Wang, H., Matthews, M., Bradford, W., Bennetzen, J. L., and Jones, A. M. (2012) G protein activation without a GEF in the plant kingdom. *PLoS Genet.* **8,** e1002756
3. Sprang, S. R. (1997) G protein mechanisms: insights from structural analysis. *Annu. Rev. Biochem.* **66,** 639–678
4. Chen, J.-G., Willard, F. S., Huang, J., Liang, J., Chasse, S. A., Jones, A. M., and Siderovski, D. P. (2003) A seven-transmembrane RGS protein that modulates plant cell proliferation. *Science* **301,** 1728–1731
5. Urano, D., Chen, J.-G., Botella, J. R., and Jones, A. M. (2013) Heterotrimeric G protein signalling in the plant kingdom. *Open Biol.* **3,** 120186
6. Reiter, E., and Lefkowitz, R. J. (2006) GRKs and β-arrestins: roles in receptor silencing, trafficking and signaling. *Trends Endocrinol. Metab.* **17,** 159–165
7. Fu, Y., Lim, S., Urano, D., Tunc-Ozdemir, M., Phan, N. G., Elston, T. C., and Jones, A. M. (2014) Reciprocal encoding of signal intensity and duration in a glucose-sensing circuit. *Cell.* **156,** 1084–1095
8. Urano, D., Phan, N., Jones, J. C., Yang, J., Huang, J., Grigston, J., Taylor, J. P., and Jones, A. M. (2012) Endocytosis of the seven-transmembrane RGS1 protein activates G-protein-coupled signalling in *Arabidopsis*. *Nat. Cell Biol.* **14,** 1079–1088
9. Urano, D., and Jones, A. M. (2014) Heterotrimeric G protein-coupled signaling in plants. *Annu. Rev. Plant Biol.* **65,** 365–384
10. Zulawski, M., and Schulze, W. X. (2015) The plant kinome. *Methods Mol. Biol.* **1306,** 1–23
11. Diévart, A., and Clark, S. E. (2004) LRR-containing receptors regulating plant development and defense. *Development* **131,** 251–261
12. Shiu, S. H., and Bleecker, A. B. (2003) Expansion of the receptor-like kinase/Pelle gene family and receptor-like proteins in *Arabidopsis*. *Plant Physiol.* **132,** 530–543
13. Llorente, F., Alonso-Blanco, C., Sánchez-Rodriguez, C., Jorda, L., and Molina, A. (2005) ERECTA receptor-like kinase and heterotrimeric G protein from *Arabidopsis* are required for resistance to the necrotrophic fungus Plectosphaerella cucumerina. *Plant J.* **43,** 165–180
14. Liu, J., Ding, P., Sun, T., Nitta, Y., Dong, O., Huang, X., Yang, W., Li, X., Botella, J. R., and Zhang, Y. (2013) Heterotrimeric G proteins serve as a converging point in plant defense signaling activated by multiple receptor-like kinases. *Plant Physiol.* **161,** 2146–2158
15. Zhang, W., He, S. Y., and Assmann, S. M. (2008) The plant innate immunity response in stomatal guard cells invokes G-protein-dependent ion channel regulation. *Plant J.* **56,** 984–996
16. Bommert, P., Je, B. I., Goldshmidt, A., and Jackson, D. (2013) The maize Gα gene *COMPACT PLANT2* functions in CLAVATA signalling to control shoot meristem size. *Nature* **502,** 555–558
17. Ishida, T., Tabata, R., Yamada, M., Aida, M., Mitsumasu, K., Fujiwara, M., Yamaguchi, K., Shigenobu, S., Higuchi, M., Tsuji, H., Shimamoto, K., Hasebe, M., Fukuda, H., and Sawa, S. (2014) Heterotrimeric G proteins control stem cell proliferation through CLAVATA signaling in *Arabidopsis*. *EMBO Rep.* **15,** 1202–1209
18. Lease, K. A., Wen, J., Li, J., Doke, J. T., Liscum, E., and Walker, J. C. (2001) A mutant *Arabidopsis* heterotrimeric G-protein β subunit affects leaf, flower, and fruit development. *Plant Cell.* **13,** 2631–2641
19. Kadota, Y., Shirasu, K., and Zipfel, C. (2015) Regulation of the NADPH oxidase RBOHD during plant immunity. *Plant Cell Physiol.* **56,** 1472–1480
20. Meng, X., and Zhang, S. (2013) MAPK cascades in plant disease resistance signaling. *Annu. Rev. Phytopathol.* **51,** 245–266
21. Torii, K. U. (2004) Leucine-rich repeat receptor kinases in plants: structure, function, and signal transduction pathways. *Int. Rev. Cytol.* **234,** 1–46
22. Mitra, S. K., Chen, R., Dhandaydham, M., Wang, X., Blackburn, R. K., Kota, U., Goshe, M. B., Schwartz, D., Huber, S. C., and Clouse, S. D. (2015) An autophosphorylation site database for leucine-rich repeat receptor-like kinases in *Arabidopsis thaliana*. *Plant J.* **82,** 1042–1060
23. Macho, A. P., Lozano-Durán, R., and Zipfel, C. (2015) Importance of tyrosine phosphorylation in receptor kinase complexes. *Trends Plant Sci.* **20,** 269–272
24. Macho, A. P., and Zipfel, C. (2014) Plant PRRs and the activation of innate immune signaling. *Mol. Cell* **54,** 263–272
25. He, K., Gou, X., Yuan, T., Lin, H., Asami, T., Yoshida, S., Russell, S. D., and Li, J. (2007) BAK1 and BKK1 regulate brassinosteroid-dependent growth and brassinosteroid-independent cell-death pathways. *Curr. Biol.* **17,** 1109–1115
26. Roux, M., Schwessinger, B., Albrecht, C., Chinchilla, D., Jones, A., Holton, N., Malinovsky, F. G., Tör, M., de Vries, S., and Zipfel, C. (2011) The *Arabidopsis* leucine-rich repeat receptor-like kinases BAK1/SERK3 and BKK1/SERK4 are required for innate immunity to hemibiotrophic and biotrophic pathogens. *Plant Cell.* **23,** 2440–2455
27. Ross, A., Yamada, K., Hiruma, K., Yamashita-Yamada, M., Lu, X., Takano, Y., Tsuda, K., and Saijo, Y. (2014) The *Arabidopsis* PEPR pathway couples local and systemic plant immunity. *EMBO J.* **33,** 62–75
28. Hok, S., Danchin, E. G. J., Allasia, V., Panabières, F., Attard, A., and Keller, H. (2011) An *Arabidopsis* (malectin-like) leucine-rich repeat receptor-like kinase contributes to downy mildew disease. *Plant. Cell Environ.* **34,** 1944–1957
29. Li, J., Wen, J., Lease, K. A., Doke, J. T., Tax, F. E., and Walker, J. C. (2002) BAK1, an *Arabidopsis* LRR receptor-like protein kinase, interacts with BRI1 and modulates brassinosteroid signaling. *Cell* **110,** 213–222
30. Nam, K. H., and Li, J. (2002) BRI1/BAK1, a receptor kinase pair mediating brassinosteroid signaling. *Cell* **110,** 203–212
31. Schulze, B., Mentzel, T., Jehle, A. K., Mueller, K., Beeler, S., Boller, T., Felix, G., and Chinchilla, D. (2010) Rapid heteromerization and phosphorylation of ligand-activated plant transmembrane receptors and their associated kinase BAK1. *J. Biol. Chem.* **285,** 9444–9451
32. Postel, S., Küfner, I., Beuter, C., Mazzotta, S., Schwedt, A., Borlotti, A., Halter, T., Kemmerling, B., and Nürnberger, T. (2010) The multifunctional leucine-rich repeat receptor kinase BAK1 is implicated in *Arabidopsis* development and immunity. *Eur. J. Cell Biol.* **89,** 169–174
33. Du, J., Gao, Y., Zhan, Y., Zhang, S., Wu, Y., Xiao, Y., Zou, B., He, K., Gou, X., Li, G., Lin, H., and Li, J. (2016) Nucleocytoplasmic trafficking is essential for BAK1- and BKK1-mediated cell-death control. *Plant J.* **85,** 520–531
34. Wang, Z., Meng, P., Zhang, X., Ren, D., and Yang, S. (2011) BON1 interacts with the protein kinases BIR1 and BAK1 in modulation of temperature-dependent plant growth and cell death in *Arabidopsis*. *Plant J.* **67,** 1081–1093
35. Gao, M., Wang, X., Wang, D., Xu, F., Ding, X., Zhang, Z., Bi, D., Cheng, Y. T., Chen, S., Li, X., and Zhang, Y. (2009) Regulation of cell death and innate immunity by two receptor-like kinases in *Arabidopsis*. *Cell Host Microbe* **6,** 34–44
36. Halter, T., Imkampe, J., Blaum, B. S., Stehle, T., and Kemmerling, B. (2014) BIR2 affects complex formation of BAK1 with ligand binding receptors in plant defense. *Plant Signal. Behav.* **9,** e28944
37. Gómez-Gómez, L., Bauer, Z., and Boller, T. (2001) Both the extracellular

leucine-rich repeat domain and the kinase activity of FSL2 are required for flagellin binding and signaling in *Arabidopsis*. *Plant Cell* **13,** 1155–1163
38. Li, B., Makino, S.-I., Beebe, E. T., Urano, D., Aceti, D. J., Misenheimer, T. M., Peters, J., Fox, B. G., and Jones, A. M. (2016) Cell-free translation and purification of *Arabidopsis thaliana* regulator of G protein signaling 1. *Protein Expr. Purif.* **126,** 33–41
39. Adjobo-Hermans, M. J. W., Goedhart, J., and Gadella, T. W., Jr. (2006) Plant G protein heterotrimers require dual lipidation motifs of Gα and Gγ and do not dissociate upon activation. *J. Cell Sci.* **119,** 5087–5097
40. Johnston, C. A., Taylor, J. P., Gao, Y., Kimple, A. J., Grigston, J. C., Chen, J.-G., Siderovski, D. P., Jones, A. M., and Willard, F. S. (2007) GTPase acceleration as the rate-limiting step in *Arabidopsis* G protein-coupled sugar signaling. *Proc. Natl. Acad. Sci. U.S.A.* **104,** 17317–17322
41. Chinchilla, D., Bauer, Z., Regenass, M., Boller, T., and Felix, G. (2006) The *Arabidopsis* receptor kinase FLS2 binds flg22 and determines the specificity of flagellin perception. *Plant Cell* **18,** 465–476
42. Lee, S.-M., Booe, J. M., and Pioszak, A. A. (2015) Structural insights into ligand recognition and selectivity for classes A, B, and C GPCRs. *Eur. J. Pharmacol.* **763,** 196–205
43. Duc, N. M., Kim, H. R., and Chung, K. Y. (2015) Structural mechanism of G protein activation by G protein-coupled receptor. *Eur. J. Pharmacol.* **763,** 214–222
44. Urano, D., and Jones, A. M. (2013) "Round up the usual suspects": a comment on nonexistent plant GPCRs. *Plant Physiol.* **161,** 1097–1102
45. Oliviusson, P., Heinzerling, O., Hillmer, S., Hinz, G., Tse, Y. C., Jiang, L., and Robinson, D. G. (2006) Plant retromer, localized to the prevacuolar compartment and microvesicles in *Arabidopsis*, may interact with vacuolar sorting receptors. *Plant Cell* **18,** 1239–1252
46. Wang, Y., Li, Z., Liu, D., Xu, J., Wei, X., Yan, L., Yang, C., Lou, Z., and Shui, W. (2014) Assessment of BAK1 activity in different plant receptor-like kinase complexes by quantitative profiling of phosphorylation patterns. *J. Proteomics.* **108,** 484–493
47. Wang, X., Kota, U., He, K., Blackburn, K., Li, J., Goshe, M. B., Huber, S. C., and Clouse, S. D. (2008) Sequential transphosphorylation of the BRI1/BAK1 receptor kinase complex impacts early events in brassinosteroid signaling. *Dev. Cell* **15,** 220–235
48. Torres, M. P., Clement, S. T., Cappell, S. D., and Dohlman, H. G. (2011) Cell cycle-dependent phosphorylation and ubiquitination of a G protein α subunit. *J. Biol. Chem.* **286,** 20208–20216
49. Clement, S. T., Dixit, G., and Dohlman, H. G. (2013) Regulation of yeast G protein signaling by the kinases that activate the AMPK homolog Snf1. *Sci. Signal.* **6,** ra78
50. Nürnberg, B., Harhammer, R., Exner, T., Schulze, R. A., and Wieland, T. (1996) Species- and tissue-dependent diversity of G-protein β subunit phosphorylation: evidence for a cofactor. *Biochem. J.* **318,** 717–722
51. Liang, X., Ding, P., Lian, K., Wang, J., Ma, M., Li, L., Li, L., Li, M., Zhang, X., Chen, S., Zhang, Y., and Zhou, J.-M. (2016) *Arabidopsis* heterotrimeric G proteins regulate immunity by directly coupling to the FLS2 receptor. *Elife.* **5,** e13568
52. Tunc-Ozdemir, M., Fu, Y., and Jones, A. M. (2016) Cautions in measuring *in vivo* interactions using FRET and BiFC in *Nicotiana benthamiana*. *Methods Mol. Biol.* **1363,** 155–174
53. Zipfel, C., Robatzek, S., Navarro, L., Oakeley, E. J., Jones, J. D. G., Felix, G., and Boller, T. (2004) Bacterial disease resistance in *Arabidopsis* through flagellin perception. *Nature* **428,** 764–767
54. Kassel, K. M., Au, D. R., Higgins, M. J., Hines, M., and Graves, L. M. (2010) Regulation of human cytidine triphosphate synthetase 2 by phosphorylation. *J. Biol. Chem.* **285,** 33727–33736